Efficient Dual-Wavelength Synchronously Mode-Locked Picosecond Laser Operating on the $^4F_{3/2} \rightarrow {}^4I_{11/2}$ Transition With Compactly Combined Dual Gain Media

Yu-Jen Huang, Ying-Shuen Tzeng, Cheng-Yu Tang, and Yung-Fu Chen

***Abstract*—A novel concept based on the dual gain media is originally proposed for achieving a compact efficient dual-wavelength synchronously mode-locked diode-end-pumped Nd laser on the $^4F_{3/2} \rightarrow {}^4I_{11/2}$ transition. We theoretically and experimentally realize that the output power ratio between two spectral outputs could be flexibly controlled simply by varying the waist position of the pump beam inside the composite gain medium. With the developed tactic, the total output power at 1.06 μm for balancing two-color intensities reaches 2.9 W. Moreover, suppressing the excitation of a few high-order transverse modes enables a fairly stable picosecond pulse train to be achieved with the self mode locking, where the mode-locked pulse width and repetition rate are measured to be 47 ps and 2.86 GHz, respectively. A series of 0.32 THz ultrashort pulses with the effective duration of 1.6 ps is further generated through the optical beating between two carrier frequencies of dual-wavelength synchronous pulses.**

***Index Terms*—Dual-wavelength generation, diode-pumped laser, mode-locked laser, optical beating.**

I. Introduction

DUAL-wavelength light sources are of great importance for a number of applications such as biomedicine, precision metrology, differential analysis, pump-probe measurement, spectroscopic study, and so on [1]. They are also desirable for producing coherent terahertz (THz) radiation through difference frequency generation, which is recognized as a powerful tool in military fields, as well as scientific studies because of its unique optical properties [2]–[4]. Nd-doped laser materials, due to the relatively strong splitting of Stark levels on the $^4F_{3/2} \rightarrow {}^4I_{11/2}$ transition, have been identified to be potentially suitable for the dual-wavelength generation.

However, the main challenge in acquiring a stable dual-wavelength operation is the gain competition between each emission line. Consequently, the optical resonator usually needs to be deliberately designed, which makes the whole laser system rather complicated and bulky [5]–[9]. Another method is to directly utilize the so-called disorder crystals as the gain media, which are characterized by various sharp fluorescent peaks with comparable intensities thanks to the random distributions of Nd ions in the crystalline sites [10]–[13]. Nevertheless, the uncontrollable intensities from such kind of lasers between each emission component usually limit their use in many practical applications. Therefore, it is highly valuable to develop a convenient and straightforward approach for readily constructing a compact dual-wavelength laser with the large degree of manipulation.

Recently, a reliable self-mode-locked operation in diode-pumped solid-state laser systems with multi-gigahertz (GHz) pulse repetition rates has been widely demonstrated with the combined effect of the Kerr lens and thermal lens [14]–[17]. In this paper, we originally propose a compact dual-wavelength picosecond diode-end-pumped Nd-doped vanadate laser with the self mode locking. The novelty relies on the fact that the Nd:YVO_4 and Nd:$GdVO_4$ crystals are physically combined to form a composite gain medium for simultaneous two-color emissions at 1064 and 1063 nm. We theoretically analyze and experimentally confirm that the output power ratio between the 1064- and 1063-nm lines could be flexibly controlled from 0.12 to 48 by varying the waist position of the pump beam. With the developed tactic, the total output power as high as 2.9 W at 1.06 μm is efficiently generated under the optimally balanced dual-wavelength operation at an incident pump power of 14 W. The influence of the waist position of the pump beam on the mode-locked performance is also systematically explored. With an intracavity aperture to suppress the excitation of a few high-order transverse modes, a stable self-mode-locked state could be achieved with the pulse duration of 47 ps and repetition rate of 2.86 GHz, respectively. We further experimentally find that the perfect temporal overlapping between the two-color pulses leads the autocorrelation trace to exhibit a strong interference fringe pattern, in which a train of optically beat pulses with the ultrahigh pulse repetition rate of 0.32 THz is effectually produced with the effective duration as short as 1.6 ps. By combining two active media with proper wavelength separation, we believe that the proposed method here is a promising way to generate a series of high-quality optically beat subpicosecond pulses with the THz repetition rate.

Manuscript received March 31, 2014; revised May 6, 2014; accepted April 30, 2014. This work was supported by the National Science Council under Grant NSC-100-2628-M-009-001-MY3.

Y.-J. Huang, Y.-S. Tzeng, and C.-Y. Tang are with the Department of Electrophysics, National Chiao Tung University, Hsinchu 30010, Taiwan (e-mail: yujenhuang@nctu.edu.tw; ystzeng.ep99g@nctu.edu.tw; tangjohnyo.ep96@g2.nctu.edu.tw).

Y.-F. Chen is with the Department of Electrophysics and the Department of Electronics Engineering, National ChiaoTung University, Hsinchu 30010, Taiwan (e-mail: yfchen@cc.nctu.edu.tw).

Color versions of one or more of the figures in this paper are available online at http://ieeexplore.ieee.org.

Digital Object Identifier 10.1109/JSTQE.2014.2324758

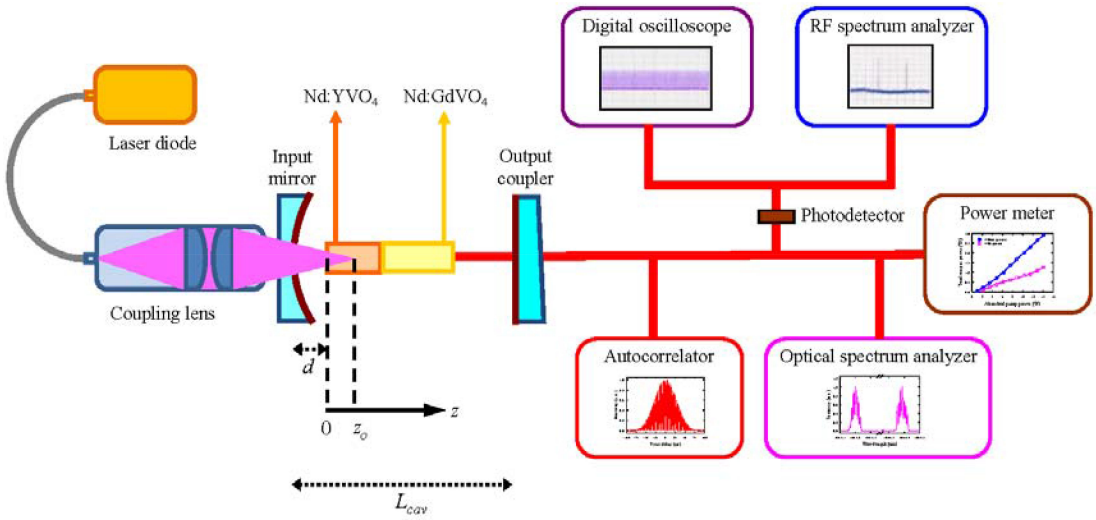

Fig. 1. Experimental configuration of the dual-wavelength self-mode-locked diode-end-pumped Nd-doped vanadate laser.

II. Experimental Setup

Fig. 1 schematically depicts the experimental configuration of our dual-wavelength self-mode-locked diode-end-pumped Nd-doped vanadate laser. A plano-concave mirror with the radius of curvature of 1000 mm was used as the input mirror, where the plane side was coated for anti-reflection at 808 nm, and the concave side was coated for high transmission at 808 nm as well as for high reflection at 1.06 μm. The composite gain medium consisted of two vanadate laser materials. The first one was a 0.2% doping a-cut Nd:YVO_4 crystal with the dimension of 3 mm $\times$ 3 mm $\times$ 5.5 mm, and it was tightly followed by a 0.5% doping a-cut Nd:$GdVO_4$ crystal with the size of 3 mm $\times$ 3 mm $\times$ 8 mm. The Nd:$GdVO_4$ crystal was arranged with its crystallographic c axis to be parallel to that of the Nd:YVO_4 crystal. All end faces of the vanadate crystals were coated for anti-reflection at the pump and lasing wavelengths. The composite gain medium was wrapped with indium foil and mounted in a water-cooled copper holder, where the temperature was maintained at 16 °C. A fiber-coupled laser diode was employed as the pump source with the nominal power of 16 W at 808 nm. The core diameter and numerical aperture of the coupling fiber were 200 μm and 0.22, respectively. For the purpose of the pump absorption of the Nd:YVO_4 crystal to be around 50%, the emission wavelength was intentionally tuned to 805 nm instead of the commonly used 808-nm line by altering the temperature of the laser diode. The residual pump light was subsequently absorbed by the followed Nd:$GdVO_4$ crystal. It is worthwhile to mention that the positions for the Nd:YVO_4 and Nd:$GdVO_4$ crystals could be exchanged in principle as long as the pump absorptions for each laser material are suitably controlled to be around 50%. Two plano-convex lenses with focal lengths of 25 mm and the total coupling efficiency of 88% were utilized to reimage the pump beam into the composite gain medium with the spot radius of 120 μm. The module of the coupling system was placed on a linear translation stage to change the waist position of the pump beam through the parameter z_o, which is defined as the distance from the entrance face of the Nd:YVO_4 crystal to the waist location of the pump beam inside the composite gain medium, as indicated in Fig. 1. A flat wedged mirror with the reflectivity of 95% at 1.06 μm was employed as the output coupler. The geometrical length of the laser cavity $L_{\rm cav}$ was set to be 36 mm for obtaining a compact self-mode-locked laser. Considering the refractive indices of the laser materials, the optical cavity length was evaluated to be approximately 52.5 mm, corresponding to the fundamental pulse repetition rate of 2.86 GHz. By controlling the number of the longitudinal modes via the spatial hole burning effect [18], the separation between the input mirror and entrance surface of the Nd:YVO_4 crystal d was fixed to be 8 mm for acquiring comparable mode-locked pulse durations at 1064 and 1063 nm. For this experimental condition, $\sim$7 longitudinal modes for each emission line oscillate, and the influence of the spatial hole burning effect on the performance of present dual-wavelength mode-locked laser is under investigation.

The spectral information of the laser output was recorded by a Fourier optical spectrum analyzer (Advantest, Q8347) with the resolution of 0.003 nm. The real-time temporal behavior of the mode-locked pulses was monitored by a high-speed InGaAs photodetector with the rise time of 35 ps, and the received signal was sent to a digital oscilloscope (Agilent, DSO 80000) with the electrical bandwidth of 12 GHz and the sampling rate of 25 ps. The output signal of the photodetector was also delivered to a RF spectrum analyzer (Advantest, R3265A) with the bandwidth of 8 GHz. A commercial autocorrelator (APE pulse check, Angewandte Physik, and Elektronik GmbH) was employed to measure the fine structure of the mode-locked pulses.

III. Theoretical Analysis

Based on the space-dependent rate equation analysis [19], [20], the pump threshold $P{\rm th}$, the slope efficiency S_e, and the output power $P_{\rm out}$ of a diode-end-pumped solid-state laser for

specific emission line can be expressed as:

$$P_{\mathrm{th},i} = \frac{\ln\left(\frac{1}{R_{\mathrm{OC},i}}\right) + L_i}{2l_{\mathrm{cry},i}\eta_{Q,i}} I_{\mathrm{sat},i}\frac{\lambda_i}{\lambda_p} V_{\mathrm{eff},i} \tag{1}$$

$$S_{e,i} = \frac{\ln\left(\frac{1}{R_{\mathrm{OC},i}}\right)}{\ln\left(\frac{1}{R_{\mathrm{OC},i}}\right) + L_i}\eta_{Q,i}\frac{\lambda_p}{\lambda_i}\eta_{o,i} \tag{2}$$

$$P_{\mathrm{out},i} = S_{e,i}\left(P_{\mathrm{in},i} - P_{\mathrm{th},i}\right), \quad i = 1, 2, \tag{3}$$

where the subscripts 1 and 2 denote the corresponding quantities for the Nd:YVO_4 crystal at $\lambda_1 = 1064$ nm and for the Nd:$GdVO_4$ crystal at $\lambda_2 = 1063$ nm, $R_{\mathrm{OC},i}$ is the reflectivity of the output coupler, L_i is the round-trip dissipative loss of the resonator, $l_{\mathrm{cry},i}$ is the crystal length, $\eta_{Q,i}$ is the quantum efficiency for the corresponding transition, $I_{\mathrm{sat},i}$ is the laser saturation intensity, λ_p is the pump wavelength, and $P_{\mathrm{th},i}$ is the incident pump power. The effective mode volume $V_{\mathrm{eff},i}$ and overlapping efficiency $\eta_{o,i}$ are given by

$$V_{\mathrm{eff},i} = \left[\iiint S_i(r,z)R_i(r,z)dv\right]^{-1} \tag{4}$$

$$\eta_{o,i} = \frac{\left[\iiint S_i(r,z)R_i(r,z)dv\right]^2}{\iiint S_i^2(r,z)R_i(r,z)dv} \tag{5}$$

where $S_i(r,z)$ is the normalized cavity mode intensity distribution and $R_i(r,z)$ is the normalized pump intensity distribution in the active medium. On the one hand, $S_i(r,z)$ for a single fundamental transverse TEM_{00} mode can be expressed as:

$$S_i(r,z) = \frac{2}{\pi\omega_i^2(z)l_{\mathrm{cry},i}}\exp\left(-2\frac{r^2}{\omega_i^2(z)}\right) \tag{6}$$

$$\omega_i(z) = \omega_{o,i}\sqrt{1 + \left(\frac{\lambda_i z}{\pi\omega_{o,i}^2}\right)^2} \approx \omega_{o,i} \tag{7}$$

where ω_i is the variation of the laser mode radius. Here, a constant mode radius is adopted because the variation of the cavity mode size in the gain medium is rather small. On the other hand, $R_i(r,z)$ for a fiber-coupled pump beam can be reasonably described as a top-hat distribution:

$$R_i(r,z) = \frac{\alpha_i e^{-\alpha_i(z - l_{\mathrm{cry},i-1})}}{\pi\omega_{p,i}^2(z)\left(1 - e^{-\alpha_i l_{\mathrm{cry},i}}\right)} H\left(\omega_{p,i}^2(z) - r^2\right) \times H\left(l_{\mathrm{cry},i} - z\right) H\left(z - l_{\mathrm{cry},i-1}\right) \tag{8}$$

$$\omega_{p,i}(z) = \omega_{\mathrm{po}}\sqrt{1 + \left(\frac{M^2\lambda_p(z - z_o)}{n_i\pi\omega_{\mathrm{po}}^2}\right)^2} \tag{9}$$

where α_i is the pump absorption coefficient at λ_p, n_i is the refractive index, $\omega_{p,i}$ is the variation of the pump radius, where the pump beam waist ω_{po} is assumed to locate at a distance z_o from the entrance of the first laser crystal and the point $z = 0$ is taken to be at the entrance surface of the composite gain medium, M^2 is the pump beam quality factor, and $H()$ is the Heaviside step function. Note that we intentionally introduce a null parameter $l_{\mathrm{cry},0}$ for the general expression of $R_i(r,z)$.

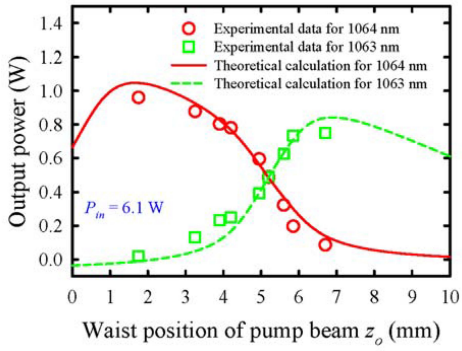

Fig. 2. Theoretical and experimental results of the output powers for 1064 and 1063 nm as a function of the waist position of the pump beam for the case of $P_{\mathrm{in}} = 6.1$ W, corresponding to $P_{\mathrm{in},1} = 2.95$ W and $P_{\mathrm{in},2} = 3.15$ W.

Substituting (6) and (8) into (4) and (5), the effective mode volume and overlapping efficiency can be rewritten as:

$$V_{\mathrm{eff},i} = \left[\frac{F\left(l_{\mathrm{cry},i-1}, l_{\mathrm{cry},i-1} + l_{\mathrm{cry},i}, \omega_i, \omega_{p,i}, \alpha_i\right)}{l_{\mathrm{cry},i}\pi\left(1 - e^{-\alpha_i l_{\mathrm{cry},i}}\right)}\right]^{-1} \tag{10}$$

$$\eta_{o,i} = \frac{\omega_i^2\left[F\left(l_{\mathrm{cry},i-1}, l_{\mathrm{cry},i-1} + l_{\mathrm{cry},i}, \omega_i, \omega_{p,i}, \alpha_i\right)\right]^2}{\left(1 - e^{-\alpha_i l_{\mathrm{cry},i}}\right)F\left(l_{\mathrm{cry},i-1}, l_{\mathrm{cry},i-1} + l_{\mathrm{cry},i}, \frac{\omega_i}{\sqrt{2}}, \alpha_i\right)} \tag{11}$$

$$F(a,b,\omega,\omega_p,\alpha) = \alpha\int_a^b\left(1 - e^{-2\frac{\omega_p^2}{\omega^2}}\right)\frac{e^{-\alpha(z-a)}}{\omega_p^2}dz \tag{12}$$

with the following experimental parameters: λ_p 805 nm, $R_{\mathrm{OC},1} = R_{\mathrm{OC},2} = 0.95$, $L_1 = L_2 = 0.003$, $\omega_1 = 190\ \mu$m, $\omega_2 = 180\ \mu$m, $\Omega_{\mathrm{po}} = 120\,\mu$m, $M^2 = 200$, $\alpha_1 = 0.12$ mm^{-1}, $\alpha_2 = 0.14$ mm^{-1}, $l_{\mathrm{cry},0} = 0$ mm, $l_{\mathrm{cry},1} = 5.5$ mm, $l_{\mathrm{cry},2} = 8$ mm, $I_{\mathrm{sat},1} = 7.473\,\mathrm{W/mm^2}$, $I_{\mathrm{sat},2} = 25.9\,\mathrm{W/mm^2}$, $n_1 = 2.222$, $n_2 = 2.249$, $\eta_{Q,1} = \eta_{Q,2} = 1$, and the variations of the output powers for 1064 and 1063 nm could be calculated as a function of the waist position of the pump beam z_o. The computed results for the case of $P_{\mathrm{in}} = 6.1$ W, corresponding to $P_{\mathrm{in},1} = 2.95$ W and $P_{\mathrm{in},2} = 3.15$ W, are illustrated in Fig. 2. It can be apparently deduced that by increasing the waist position of the pump beam from 2 to 7 mm, the output powers at 1064 and 1063 nm would monotonously reduced and raised, respectively. This indicates that the output power ratio between two spectral outputs could be flexibly controlled just by varying the waist position of the pump beam, which will be experimentally verified in the following section.

IV. Performance of the Dual-Wavelength Self-Mode-Locked Laser

First of all, a stable continuous-wave self-mode-locked state in present Nd-doped vanadate laser could be accomplished by finely tilting the composite gain medium and carefully adjusting the cavity alignment, as observed in our previous works [14]–[16]. Note that once the incident pump power reached the threshold for oscillation, the laser could instantaneously step into the stable self-mode-locked state. Then, we

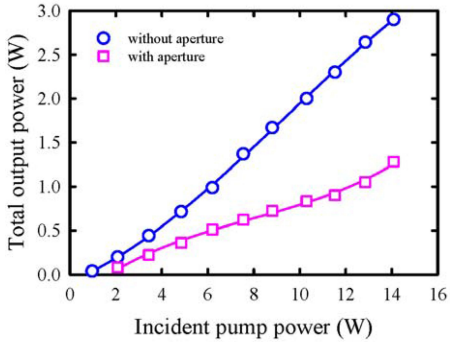

Fig. 3. Dependence of the total output power at 1.06 μm with and without an intracavity aperture on the incident pump power under the optimally balanced dual-wavelength intensities, corresponding to the case of $zo = 5.2\,\mathrm{mm}$.

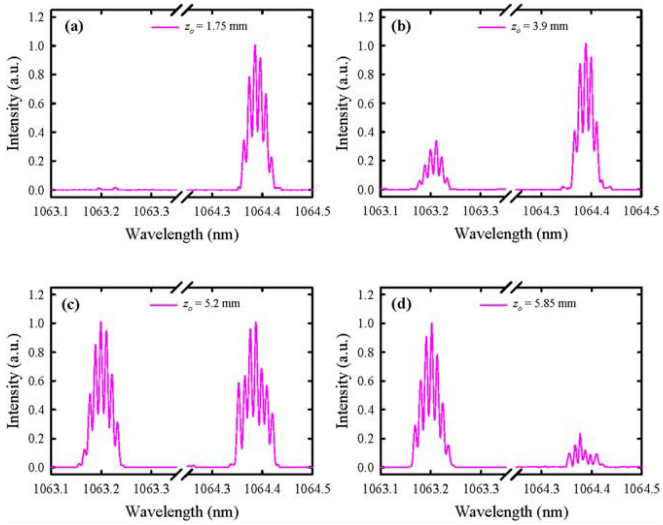

Fig. 4. Optical spectra for the dual-wavelength self-mode-locked laser: (a) $zo = 1.75$ mm, (b) $zo = 3.9$ mm, (c) $zo = 5.2$ mm, and (d) $zo = 5.85$ mm.

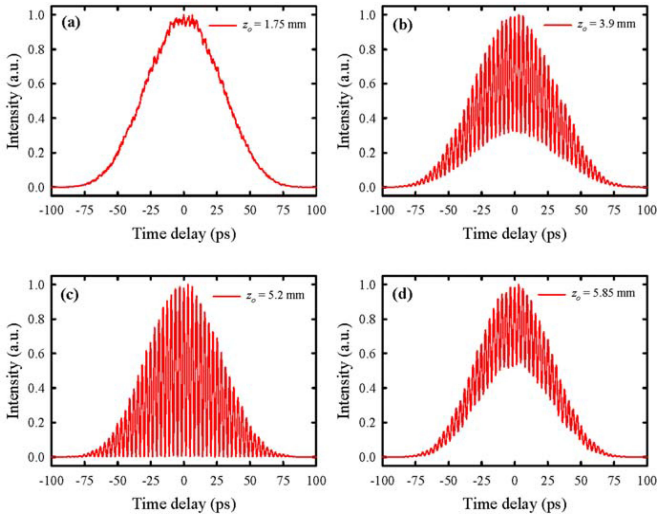

Fig. 5. Autocorrelation traces for the dual-wavelength self-mode-locked laser: (a) $z_o = 1.75$ mm, (b) $z_o = 3.9$ mm, (c) $z_o = 5.2$ mm, and (d) $z_o = 5.85$ mm.

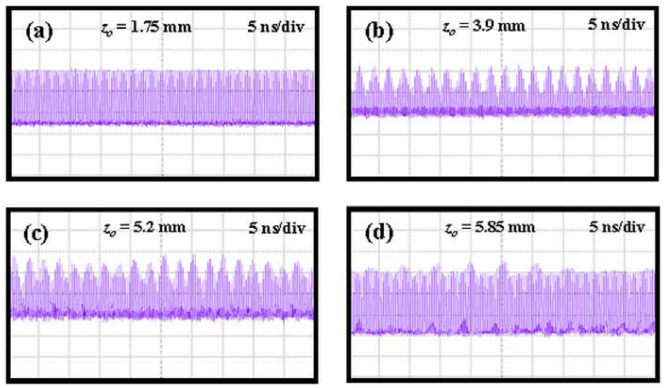

Fig. 6. Oscilloscope traces for the dual-wavelength self-mode-locked laser: (a) $z_o = 1.75$ mm, (b) $z_o = 3.9$ mm, (c) $z_o = 5.2$ mm, and (d) $z_o = 5.85$ mm.

varied the waist position of the pump beam along the optical axis of the resonator to measure the output powers radiated from the Nd:YVO_4 and Nd:$GdVO_4$ crystals at an incident pump power of 6.1 W, as displayed in Fig. 2. Here, the ratio of the spectral peak intensities for each emission line was used to determine the output powers for 1064 and 1063 nm after the total output power was recorded at different waist position of the pump beam. Experimental results could be found to agree excellently with the theoretical prediction in Section III. By continuously varying the waist position of the pump beam from 1.75 to 6.7 mm, the output powers are experimentally found to change from 0.96 to 0.09 W for 1064 nm and from 0.02 to 0.75 W for 1063 nm. As a result, the output power ratio $P_{1064\,\mathrm{nm}}/P_{1063\,\mathrm{nm}}$ could be continuously altered from 48 to 0.12 when the waist position of the pump beam is gradually increased from 1.75 to 6.7 mm. Fig. 3 illustrates the dependence of the total output power at 1.06 μm on the incident pump power under the optimally balanced dual-wavelength intensities, corresponding to the case for $z_o = 5.2\,\mathrm{mm}$. At an incident pump power of 14 W, the maximum total output power as high as 2.9 W is generated with our developed dual-wavelength mode-locked miniature laser. The corresponding optical conversion and slope efficiencies are evaluated to be approximately 21 and 22.3%, respectively. Fig. 4(a)–(d) depict the optical spectra at an incident pump power of 10.3 W for the cases of $z_o = 1.75$, 3.9, 5.2, and 5.85 mm. The central wavelengths for each spectral band locate at 1063.18 and 1064.38 nm, respectively. Besides, the longitudinal modes could be clearly resolved, and the measured mode spacing of 0.01 nm is consistent with the theoretical value of 0.011 nm [15]. The corresponding autocorrelation traces for the cases of $z_o = 1.75$, 3.9, 5.2, and 5.85 mm are exhibited in Fig. 5(a)–(d). Experimental results undoubtedly confirm that our dual-wavelength self-mode-locked laser is in a perfect synchronization status. As a consequence, an interference pattern could be clearly observed due to the optical beating between two carrier frequencies of the dual-wavelength mode-locked pulses [21]–[23]. More intriguingly, as the output power ratio is

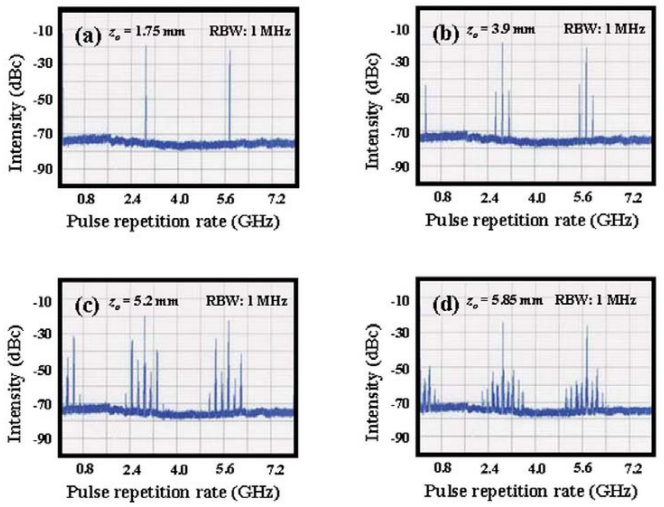

Fig. 7. RF spectra for the dual-wavelength self-mode-locked laser: (a) $z_o = 1.75$ mm, (b) $z_o = 3.9$ mm, (c) $z_o = 5.2$ mm, and (d) $z_o = 5.85$ mm.

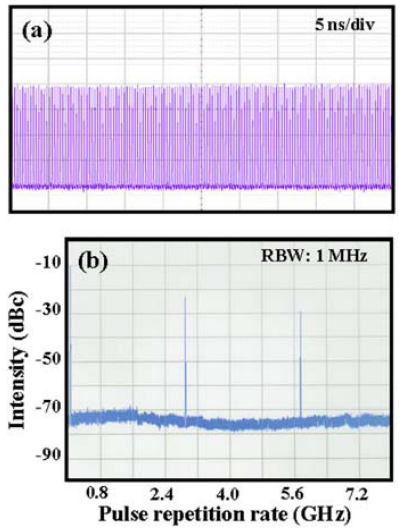

Fig. 8. (a) Oscilloscope trace, and (b) RF spectrum, for the dual-wavelength self-mode-locked laser with the pure TEM00 mode oscillation for the case of $z_o = 5.2$ mm.

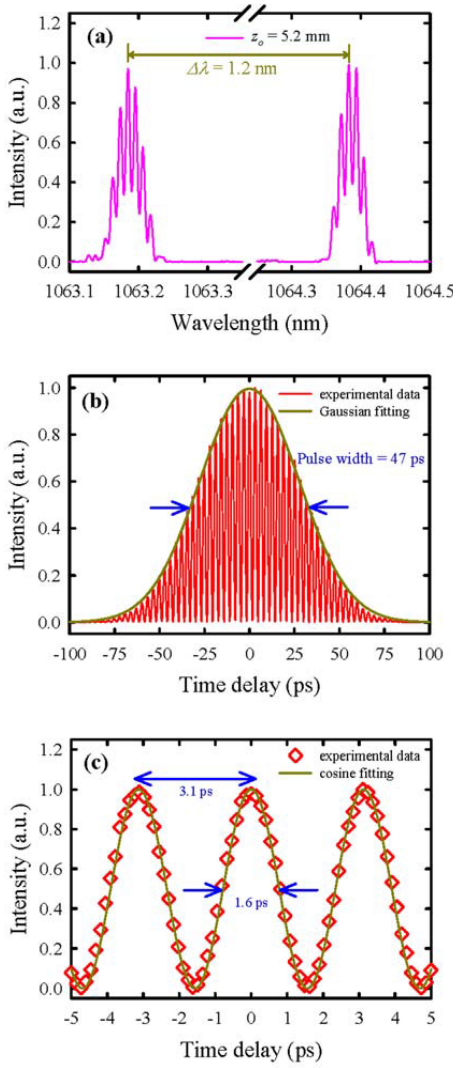

Fig. 9. (a) Optical spectrum for the dual-wavelength self-mode-locked laser with the pure TEM_{00} mode oscillation for the case of $z_o = 5.2$ mm; corresponding autocorrelation traces with the time span of (a) 200 ps and (b) 10 ps.

equal to unity, a high-quality quasi-periodic optically beat pulse train could be generated with the modulation depth of 100%, as described in Fig. 5(c). Note that the dual-wavelength mode-locked pulses are found to be always synchronous during the experiment.

Typical oscilloscope traces of the dual-wavelength mode-locked pulses at an incident pump power of 10.3 W for the cases of $z_o = 1.75$, 3.9, 5.2, and 5.85 mm are illustrated in Fig. 6(a)–(d) with the time span of 50 ns. The corresponding RF spectra for the cases of $z_o = 1.75$, 3.9, 5.2, and 5.85 mm are also displayed in Fig. 7(a)–(d). Although the perfect temporal overlapping between the dual-wavelength mode-locked pulses has been verified in the autocorrelation measurement, the pulse train is experimentally found to be modulated by the beat frequency between the transverse modes [24], which is resulted from the defocusing pumping in the end-pumped configuration. By increasing the waist position of the pump beam, more transverse modes would be excited, as can be indicated in Fig. 7. The degree of the modulation depth of the pulse train depends on the number of the excited transverse modes. When more transverse modes are involved, the averaging effect for the contribution of all transverse modes would initially cause the temporal behavior to exhibit a regular envelop modulation of the pulse train, and then, to display a relatively irregular envelop of the pulse train with small modulation depth, as can be seen in Fig. 6. In fact, the laser would display a complex spatio-temporal dynamics at this time when different transverse position of the output beam was measured [25]. To suppress the excitation of a few high-order transverse modes, an intracavity aperture was inserted inside the cavity [26]. Consequently, a quite stable pulse train with the amplitude fluctuation better than 2% was obtained, as shown in Fig. 8(a). The stability could also be confirmed with the RF spectrum displayed in Fig. 8(b). The peak of the fundamental

harmonics is 50 dBc above the background level, and the value $\Delta\nu/\nu$ is estimated to be around 10^{-4} over an hour-long operation, which indicates an excellent long-term stability. Here, the relative frequency deviation of the fundamental harmonic $\Delta\nu/\nu$ is introduced to quantitatively characterize the stability of the laser, where ν is the central frequency and $\Delta\nu$ is the full width at half maxima (FWHM) of the fundamental harmonic, respectively. Note that the insertion of an intracavity aperture would accompany with the expense of the decreased output power, where the maximum value becomes 1.3 W, as shown in Fig. 3.

Fig. 9(a) and (b) describes the optical spectrum and autocorrelation trace for the balanced dual-wavelength operation with the pure TEM_{00} mode oscillation, which are similar to the results in Figs. 4(c) and 5(c). The FWHM of the autocorrelation trace is measured to be about 68 ps. If the temporal intensity of the Gaussian-shaped profile is assumed, the pulse duration could thus be evaluated as 47 ps. The detailed structure of the interference fringe pattern is depicted in Fig. 9(c) with the time span of 10 ps. The optically beat frequency of 0.32 THz could be deduced from the pulse period of 3.1 ps, and it is consistent with the peak wavelength separation $\Delta\lambda$ of 1.2 nm of the two central spectral bands, as can be derived in Fig. 9(a). In terms of the cosine-like pulse shape, the effective pulse width of the optically beat wave could be inferred to exactly correspond to the FWHM duration of the experimentally measured autocorrelation trace [27]. As a result, the effective pulse duration is calculated to be as short as 1.6 ps, considerably shorter than the original Gaussian-shaped pulse of 47 ps. It is believed that the dual-wavelength concept presented here may be a promising means for generating THz optical wave via nonlinear frequency conversion based on the GaSe, GaP, and $ZnGeP_2$ crystals etc [28].

V. Conclusion

In summary, a novel approach has been successfully developed for efficiently generating dual-wavelength picosecond pulses in a self-mode-locked diode-end-pumped Nd laser. We have compactly joined the Nd:YVO_4 crystal to the Nd:$GdVO_4$ crystal as a composite gain medium for simultaneously emitting 1064- and 1063-nm radiations. The output powers for each spectral line as a function of the waist position of the pump beam has been properly measured to validate our theoretical prediction on the basis of the space-dependent rate equation analysis. Under the optimally balanced dual-wavelength operation, our developed laser could effectually produce the output power of up to 2.9 W. With repressing the excitation of a few high-order transverse modes, a reliable and stable train of picosecond pulses has been achieved with the pulse duration of 47 ps and repetition rate of 2.86 GHz, respectively. High-quality optically beat pulses with the 1.6 ps pulse duration and 0.32 THz repetition rate are further observed as a result of the temporal interference between the dual-wavelength synchronous pulses.

References

[1] B. M. Walsh, "Dual wavelength lasers," *Laser Phys.*, vol. 20, pp. 622–634, Mar. 2010.

[2] D. L. Woolard, E. R. Brown, M. Pepper, and M. Kemp, "Terahertz frequency sensing and imaging: A time of reckoning future applications?" *Proc. IEEE*, vol. 93, no. 10, pp. 1722–1743, Oct. 2005.

[3] M. Koch, "Terahertz technology: A land to be discovered," *Opt. Photon. News*, vol. 18, pp. 20–25, Mar. 2007.

[4] G. Kh. Kitaeva, "Terahertz generation by means of optical lasers," *Laser Phys. Lett.*, vol. 5, pp. 559–576, May 2008.

[5] M. B. Danailov and I. Y. Milev, "Simultaneous multiwavelength operation of Nd:YAG laser," *Appl. Phys. Lett.*, vol. 61, pp. 746–748, Aug. 1992.

[6] B. Wu, P. Jiang, D. Yang, T. Chen, J. Kong, and Y. Shen, "Compact dual-wavelength Nd:$GdVO_4$ laser working at 1063 and 1065 nm," *Opt. Exp.*, vol. 17, pp. 6004–6009, Aug. 2009.

[7] P. Zhao, S. Ragam, Y. J. Ding, and I. B. Zotova, "Compact and portable terahertz source by mixing two frequencies generated simultaneously by a single solid-state laser," *Opt. Lett.*, vol. 35, pp. 3979–3981, Dec. 2010.

[8] P. Zhao, S. Ragam, Y. J. Ding, and I. B. Zotova, "Power scalability and frequency agility of compact terahertz source based on frequency mixing from solid-state lasers," *Appl. Phys. Lett.*, vol. 98, p. 131106, Mar. 2011.

[9] A. A. Sirotkin, S. V. Garnov, V. I. Vlasov, A. I. Zagumennyi, Y. D. Zavartsev, S. A. Kutovoi, and I. A. Shcherbakov, "Two-frequency vanadate lasers with mutually parallel and orthogonal polarizations of radiation," *Quantum Electron.*, vol. 42, pp. 420–426, May 2012.

[10] H. Yu, H. Zhang, Z. Wang, J. Wang, Y. Yu, Z. Shi, X. Zhang, and M. Liang, "High-power dual-wavelength laser with disordered Nd:CNGG crystals," *Opt. Lett.*, vol. 34, pp. 151–153, Jan. 2009.

[11] A. Brenier, Y. Wu, P. Fu, J. Zhang, and Y. Zu, "Diode-pumped laser properties of Nd^{3+}-doped $La_2CaB_{10}O_{19}$ crystal including two-frequency generation with 4.6 THz separation," *Opt. Exp.*, vol. 17, pp. 18730–18737, Oct. 2009.

[12] Y. J. Chen, X. H. Gong, Y. F. Lin, J. H. Huang, Z. D. Luo, and Y. D. Huang, "Diode-pumped orthogonally polarized dual-wavelength Nd^{3+}:$LaBO_2MoO_4$ laser," *Appl. Phys. B*, vol. 112, pp. 55–60, Aug. 2013.

[13] Y. Zhao, S. Zhuang, X. Xu, J. Xu, H. Yu, Z. Wang, and X. Xu, "Anisotropy of laser emission in monoclinic, disordered crystal Nd:LYSO," *Opt. Exp.*, vol. 22, pp. 2228–2235, Feb. 2014.

[14] H. C. Liang, Y. J. Huang, W. C. Huang, K. W. Su, and Y. F. Chen, "High-power, diode-end-pumped, multigigahertz self-mode-locked Nd:YVO_4 laser at 1342 nm," *Opt. Lett.*, vol. 35, pp. 4–6, Jan. 2010.

[15] Y. J. Huang, H. C. Liang, Y. F. Chen, H. J. Zhang, J. Y. Wang, and M. H. Jiang, "High-power 10-GHz self-mode-locked Nd:$LuVO_4$ laser," *Laser Phys.*, vol. 21, pp. 1750–1754, Oct. 2011.

[16] Y. J. Huang, Y. S. Tzeng, C. Y. Tang, Y. P. Huang, and Y. F. Chen, "Tunable GHz pulse repetition rate operation in high-power TEM_{00}-mode Nd:YLF lasers at 1047 nm and 1053 nm with self mode locking," *Opt. Exp.*, vol. 20, pp. 18230–18237, Jul. 2012.

[17] H. Liu, J. Huang, F. Tang, J. Li, W. Weng, Y. Ge, H. Zheng, K. Ruan, F. Shi, S. Dai, J. Deng, and W. Lin, "Generation of 3.8-GHz picosecond pulses from a diode-pumped self-mode-locked Yb:YAG thin disk laser," *IEEE Photon. Technol. Lett.*, vol. 26, pp. 418–421, Feb. 2014.

[18] Y. F. Chen, Y. J. Huang, P. Y. Chiang, Y. C. Lin, and H. C. Liang, "Controlling number of lasing modes for designing short-cavity self-mode-locked Nd-doped vanadate lasers," *Appl. Phys. B*, vol. 103, pp. 841–846, Jun. 2011.

[19] T. Y. Fan and R. L. Byer, "Diode laser-pumped solid-state lasers," *IEEE J. Quantum Electron.*, vol. 24, no. 6, pp. 895–912, Jun. 1988.

[20] P. Laporta and M. Brussard, "Design criteria for mode size optimization in diode-pumped solid-state lasers," *IEEE J. Quantum Electron.*, vol. 27, no. 10, pp. 2319–2326, Oct. 1991.

[21] G. Q. Xie, D. Y. Tang, H. Luo, H. J. Zhang, H. H. Yu, J. Y. Wang, X. T. Tao, M. H. Jiang, and L. J. Qian, "Dual-wavelength synchronously mode-locked Nd:CNGG laser," *Opt. Lett.*, vol. 33, pp. 1872–1874, Aug. 2008.

[22] Z. Cong, D. Tang, W. D. Tan, J. Zhang, C. Xu, D. Luo, X. Xu, D. Li, J. Xu, X. Zhang, and Q. Wang, "Dual-wavelength passively mode-locked Nd:$LuYSiO_5$ laser with SESAM," *Opt. Exp.*, vol. 19, pp. 3984–3989, Feb. 2011.

[23] H. Xu, H. Zhang, H. Yu, D. Tang, and C. Xu, "Passive mode-locking performance of mixed Nd:$La_{0.11}Y_{0.89}VO_4$ crystal," *Opt. Exp.*, vol. 22, pp. 5350–5356, Mar. 2014.

[24] H. C. Liang, Y. J. Huang, P. Y. Chiang, and Y. F. Chen, "Highly efficient Nd:$Gd_{0.6}Y_{0.4}VO_4$ laser by direct in-band pumping at 914 nm and observation of self-mode-locked operation," *Appl. Phys. B*, vol. 103, pp. 637–641, Jun. 2011.

[25] H. C. Liang, Y. C. Lee, J. C. Tung, K. W. Su, K. F. Huang, and Y. F. Chen, "Exploring the spatio-temporal dynamics of an optically pumped semiconductor laser with intracavity second harmonic generation," *Opt. Lett*, vol. 37, pp. 4609–4611, Nov. 2012.
[26] Y. J. Huang, Y. S. Tzeng, C. Y. Tang, S. Y. Chiang, H. C. Liang, and Y. F. Chen, "Efficient high-power terahertz beating in a dual-wavelength synchronously mode-locked laser with dual gain media," *Opt. Lett.*, vol. 39, pp. 1477–1480, Mar. 2014.
[27] C. L. Wang and C. L. Pan, "Tunable multiterahertz beat signal generation from a two-wavelength laser-diode array," *Opt. Lett.*, vol. 20, pp. 1292–1294, Jun. 1995.
[28] Y. J. Ding, "High-power tunable terahertz sources based on parametric processes and applications," *IEEE J. Sel. Top. Quantum Electron.*, vol. 13, no. 3, pp. 705–720, May/Jun. 2007.

Yu-Jen Huang was born in Hualien, Taiwan, in 1987. He received the B.S. and Ph.D. degrees in electrophysics from National Chiao Tung University, Hsinchu, Taiwan, in 2009 and 2013, respectively.

He is currently a Postdoctoral Research Fellow in the Department of Electrophysics, National Chiao Tung University. His research interests include the physics and technology of diode-pumped solid-state lasers and nonlinear frequency conversion.

Dr. Huang is a Member of the Optical Society of America.

Ying-Shuen Tzeng was born in Yunlin, Taiwan, in 1984. He is currently working toward the Ph.D. degree in electrophysics with National Chiao Tung University, Hsinchu, Taiwan.

His research interests include multi-wavelength diode-pumped solid-state lasers.

Cheng-Yu Tang was born in Taichung, Taiwan, in 1989. He is currently working toward the Ph.D. degree in electrophysics with National Chiao Tung University, Hsinchu, Taiwan.

His research interests include Q-switched and mode-locked diode-pumped solid-state lasers.

Yung-Fu Chen was born in Lukang, Taiwan, in 1968. He received the B.S. and Ph.D. degrees in electronics engineering from National Chiao Tung University (NCTU), Hsinchu, Taiwan, in 1990 and 1994, respectively.

In 1994, he was with the Precision Instrument Development Center, National Science Council, Taiwan, where his research mainly concerns the development of diode-pumped solid-state laser as well as quantitative analysis in surface electron spectroscopy. In 1999, he was with NCTU as an Associate Professor in the Department of Electrophysics, where in 2001, he was promoted to the Professor. He had served as an Executive Dean in the College of Science, NCTU between 2006 and 2007. He had also served as the Chair in the Department of Electrophysics between 2011 and 2013. Since 2011, he has been identified as the Distinguished Professor. He has received several outstanding awards, such as Sun-Yet-Sen Academic Award for excellent papers in 2008, outstanding research award from National Science Council in 2004 and 2011, and outstanding Honorary Award from Ho C.T. Education Foundation in 2011. His main research includes laser physics, solid-state lasers, Q-switched lasers, mode-locked lasers, and transverse pattern formation in microchip lasers.

Dr. Chen is a Member of the Optical Society of America and the IEEE Photonics Society. Currently, he serves as the Associate Editor for the journal *Optics Express*.